

Experimental and numerical study of damage initiation mechanism in elastomeric composites

T.D. Silva Botelho ^a, E. Bayraktar ^{b,*}

^a Supmeca/LISMMA-Paris, School of Mechanical and Manufacturing Engineering, St-Ouen, France

^b Chair of Industrial Materials, CNAM, Arts et Métiers, 75141 Paris 03, France

* Corresponding author: emin.bayraktar@supmeca.fr

Received 02.02.2009; published in revised form 01.09.2009

Analysis and modelling

ABSTRACT

Purpose: Experimental and Finite Element Analysis (FEA) of the damage initiation mechanisms in elastomeric composites were carried out under static loading at room temperature. Double Cantilever Beam (DCB) specimens from natural rubber (NR) vulcanised and reinforced with other materials such as carbon black, silica, fibres and textiles or metals (rubber composites).

Design/methodology/approach: Very huge experimental results were compared with that of the Finite Element Analysis (FEA). Damage mechanism has been described with a threshold criterion to identify damage. The damage was evaluated just at the beginning of the tearing by assuming large strain. A typical type of specimen geometry of Double Cantilever Beam (DCB) specimens was considered under static tensile tests conducted on the notched specimens with variable depths.

Findings: In this stage of this research, a finite element analysis (FEA) has been applied under the same conditions of this part in order to obtain the agreement between experimental and FEA results. The numerical modelling is a representation of a previous experimental study. The specimen is stretched more than once its initial size, so that large strains occur. A hyper elastic Moonley-Rivlin law and a Griffith criterion are chosen. The finite elements analysis was performed with ABAQUS code (V.6.4.4).

Practical implications: A damage criterion was suggested in the case of simple tension conditions by assuming large strain levels. an effective finite elements model has been developed to evaluate notch size effects on the load-displacement elastic response of 3D-DCB type specimen.

Originality/value: This study proposes a threshold criterion for the damage just at the beginning of the tearing for Double Cantilever Beam (DCB) specimens from rubber composites and gives a detail discussion for explaining the damage mechanisms. Comparison of FEA results with those of experimental studies gives many facilities for the sake of simplicity in industrial applications.

Keywords: Damage mechanism; Finite elements model; Rubber composites; Comparative analysis

Reference to this paper should be given in the following way:

T.D. Silva Botelho, E. Bayraktar, Experimental and numerical study of damage initiation mechanism in elastomeric composites, Journal of Achievements in Materials and Manufacturing Engineering 36/1 (2009) 65-70.

1. Introduction

Natural rubber (NR) possesses excellent mechanical properties, including strength and elasticity, which are unmatched by synthetic rubbers. Therefore, NR is often a material of choice for manufacturing of engineering products such as tyres, bearings for bridges and buildings, anti-vibration mountings, dock-fenders and rubber weirs. However, raw NR is a tough and highly elastic material, making it difficult to process compared with synthetic rubbers. Furthermore, NR exhibits variation in properties from batch to batch. These are major disadvantages of NR which need to be corrected in order to maintain its competitiveness with synthetic rubbers [1-5].

Natural rubber (NR) can be modified, chemically or physically, in order to improve or diversify its properties. Use of a single rubber is rarely adequate for manufacturing of rubber products. This is because rubbers are usually employed in engineering applications which require demanding properties such as high strength, high modulus, high damping properties or greater wear, often at elevated temperatures or are in contact with oils. Therefore, uses of two or more rubbers (rubber blends) or reinforcement of rubbers with other materials such as carbon black, silica, fibres and textiles or metals (rubber composites) are necessary in the manufacturing of rubber products.

However, the uses of rubber blends or rubber composites are not straight forward. There are a number of problems associated with their uses. For rubber composites, adhesions between the rubbers and other materials are of paramount important in determining their properties and damage characteristics. Type and form of the materials used and their arrangement within the rubber also provide many possibilities for designing the properties of the rubber composites [6-18].

The objective of this research is to seek understanding of the origins of the damage mechanism and explaining its properties of NR by using DCB specimens undergone to static loading. Actually, some numerical difficulties arise while modelling of the elastomeric composites behaviour, first of them coming from the non-linear elasticity behaviour (hyperelastic). To evaluate damage effects on such materials, strong, full - bodied experimental data are needed and a substantial numerical effort is required.

By using a huge amount of experimental data, an effective finite elements model has been developed to evaluate notch size effects on the load-displacement elastic response of 3D-DCB type specimen. It was highlighted on the numerical efforts needed to reasonably simulate the tests and to achieve an accurate experimental-numerical correlation.

2. Experimental conditions and analysis

2.1. Material

The tested Double Cantilever Beam (DCB) specimens have been prepared by LRCP (National rubber research Institute in Paris) from natural rubber (NR) vulcanised and reinforced with other materials such as carbon black, silica, fibres and textiles or metals (rubber composites). They are hyperelastic materials. The

coefficients of the Mooney-Rivlin law were identified in previous studies [6-8] and are summarised in Table 1.

Table 1.
Hyperelastic law's coefficients

Coefficient	Value
C10	0.295788
C01	-0.018755
C20	0.014761
C11	0
C02	0
D1	0.000967
D2	0

2.2. Specimen and loading conditions

The specimen geometry is described in Figure 1. The useful part of the specimen is 150 mm long, 25 mm height, and 15 mm at the minimum. The sides of the central part have a 5 mm radius. A notch could be performed on one side of these specimens, at the symmetry plane. This notch was carried out with a lancet to ensure an initial sharp perpendicular to the loading direction.

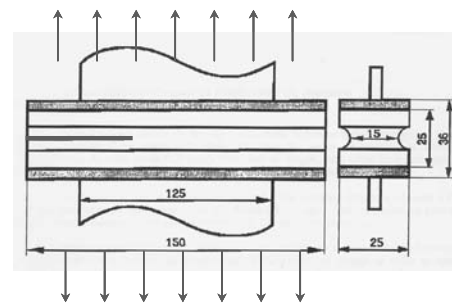


Fig. 1. Geometry of the NR-DCB specimen

All of the static tensile tests have been carried out on a Mayes hydraulic testing device attached to a computer-acquisition storing system both normal load and normal displacement. The solicitation speed was too slowly (0.25 mm/s).

2.3. Discussion of experimental results

A force vs. displacement curve has been obtained then computed for each test condition (Figure 2), and a fourth order polynomial equation fitted to all of the experimental results. With a general polynomial formula was given as follows:

$$\text{Force} = \sum_{k=1}^4 a_k (\text{displacement})^k \quad (1)$$

Coefficient a_0 is necessarily zero because no force could occur if no displacement is applied. The coefficients of the fitted curves are summarized in Table 2.

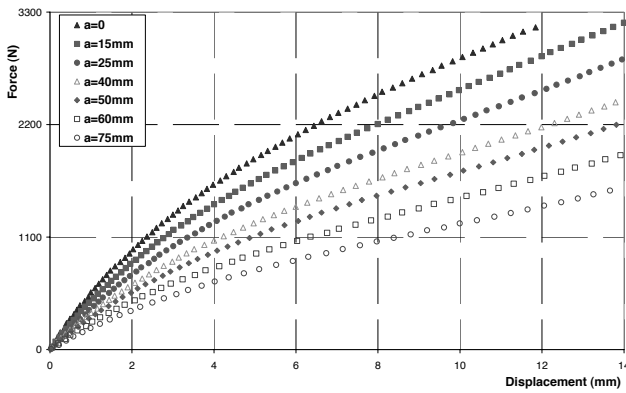


Fig. 2. Experimental force vs. displacement curves

Table 2. Coefficients of the experimental fitted force vs. displacement curves

Notch length (mm)	a_4	a_3	a_2	a_1	Correlation coefficient (R^2)
0	-0.167	5.4246	-69.643	607.58	0.9999
15	-0.091	3.5957	-53.205	517.55	1
25	-0.056	2.4885	-40.724	438.32	1
40	-0.060	2.4896	-38.09	384.85	0.9999
50	-0.049	2.0729	-32.317	338.89	0.9999
60	-0.041	1.7327	-26.634	282.96	0.9999
75	-0.026	1.1945	-19.829	227.84	1

The stiffness of the specimen is then directly obtainable from the fitted curves as their slopes. All specimens display a decreasing stiffness while increasing the loading (Figure 3). The longer the notch, the lower the stiffness is. The stiffness curves come closer while increasing the loading but they still remain significantly different. For some of the tests (unnotched and $a = 15$ mm mainly), a loss of stiffness is observed, accounting for damage.

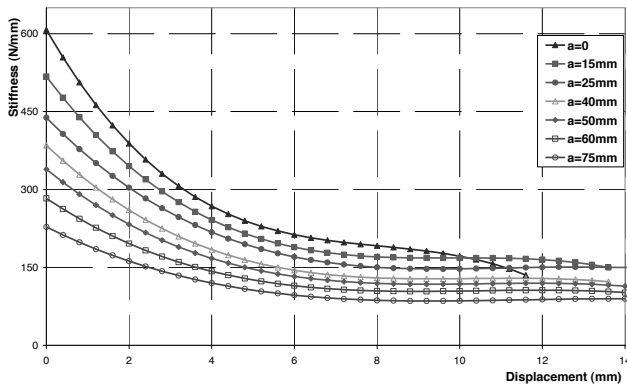


Fig. 3. Stiffness of the specimen for various notch lengths calculated from the fitted force vs. displacement curves

Such a regular behaviour could be of great interest from a non destructive control point of view: during life service of NR

components, a simple stiffness recording could serve as notch-length monitoring or damage detection.

From the coefficients (Table 2) of the fitted Force vs. Displacement curves (Eq.(1)), an expression for each a_k coefficient is computed, accounting for the notch length effect:

$$\text{Force} = \sum_{k=1}^4 a_k(a) (\text{displacement})^k \quad (2)$$

with

$$\begin{cases} a_4(a) = 1E-6.a^3 - 2E-04.a^2 + 7.3E-3.a - 0.1673 \\ a_3(a) = 7E-3.a^2 - 0,101.a + 5.1484 \\ a_2(a) = 0.6218.a - 63.601 \\ a_1(a) = -5.0203.a + 589.770 \end{cases}$$

And the correlation coefficients are 0.9862, 0.9441, 0.9411 and 0.9881 respectively.

3. Damage initiation mechanism

Damage mechanism in the DCB specimens for NR has been evaluated by Scanning Electron Microscopy (SEM) just at the beginning of the tearing in a state of plane strain. Static tensile samples were drawn only up to the beginning of the crack propagation and then stopped the machine. The samples were kept constant at this position by means of a special device having a quick locking system where special cover has been arranged and then, the entire setting is placed in SEM for the examinations. The SEM photomicrographs were carried out in a 435 VP - LEO-2003 model scanning electron microscopy (SEM).

Different stages of the crack evolution at the end of the notch in the NR-DCB specimen during uniaxial tensile test are shown in the Figure 4. It begins to open with the solicitation and takes a round shape form at the bottom of the notch. At a certain level of the deformation, the failure occurs suddenly.

The SEM photomicrographs (Figure 5a-d) show the damage initiation mechanism and/or the evolution of too early beginning of the crack propagation for the NR as a round shape form at the bottom of crack of the samples (Figures 5a-d). Crystallisation phenomenon during loading is typically observed all of the composition of the NR samples (Figure 5c-d). This phenomenon is verified in evolution of the small cavities to the final stages in the rhombus shapes. These evolutions have been observed regularly on the NR-DCB specimens studied here that explain the damage initiation mechanism under static solicitation.

Based on the above judgment, there would seem to be an optimum level of adhesion between rubber and filler for the best reinforcement, although the desired interaction may depend on the particular fracture conditions that influence the damage initiation. The results obtained on the NR-DCB samples under static loading, give a clear idea that the structure and additive elements play a major role on the fracture behaviour – failure modes of these materials. This is a basic idea to explain the damage initiation in NR composites. Thus, some interesting interactions between the structure, chains and additive elements occurred in the rubber composites can explain the evolution of the tearing and or a threshold value for the critical damage.

a)

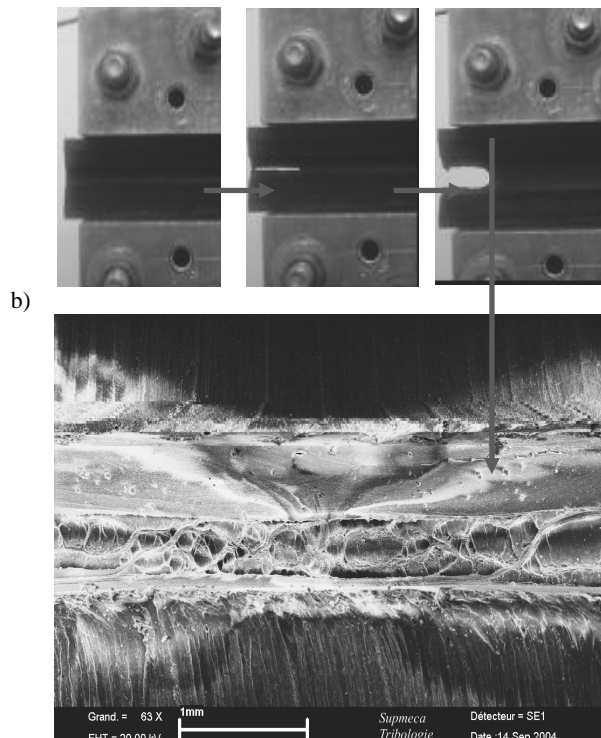


Fig. 4. Different stages of the crack evolution in the NR-DCB specimen during uniaxial tensile test, a) Formation of elliptical shape at the bottom of the notch and b) SEM photomicrograph showing the beginning of the crack propagation at this point

4. Finite Element Model

A Notch could be carried out on one side of these specimens, at the symmetry plane. The Finite Elements Model (FEM) reproduced these tests using Moonley-Rivlin hyperelastic behaviour whose coefficients were identified formerly in the LRCP-Institute [6-8]. Numerical and experimental results correlated receptively.

To investigate further the damage behaviour of the specimen, a FEM model is required, principally to evaluate in a future work the damage. Then one first has to validate the model on the actual mechanical tests. This is the main target of the present part. The FEM has been constructed according to experimental data. The ABAQUS® code was used. Only an half of the specimen has been computed and proper boundary conditions were applied because the test (specimen and loading) has a “X-Z” symmetry (from Figure 1). Figure 6 gives an example of the deformed shape of a specimen with a 50 mm length notch under a 7.37 mm applied displacement. The model results were X-Z mirrored (reflected) for sake of comprehension.

The notch has been reasonably designed according to the lancet's shape: the notch width and the lancet's tip radius were 3 mm (Figure 7).

a)

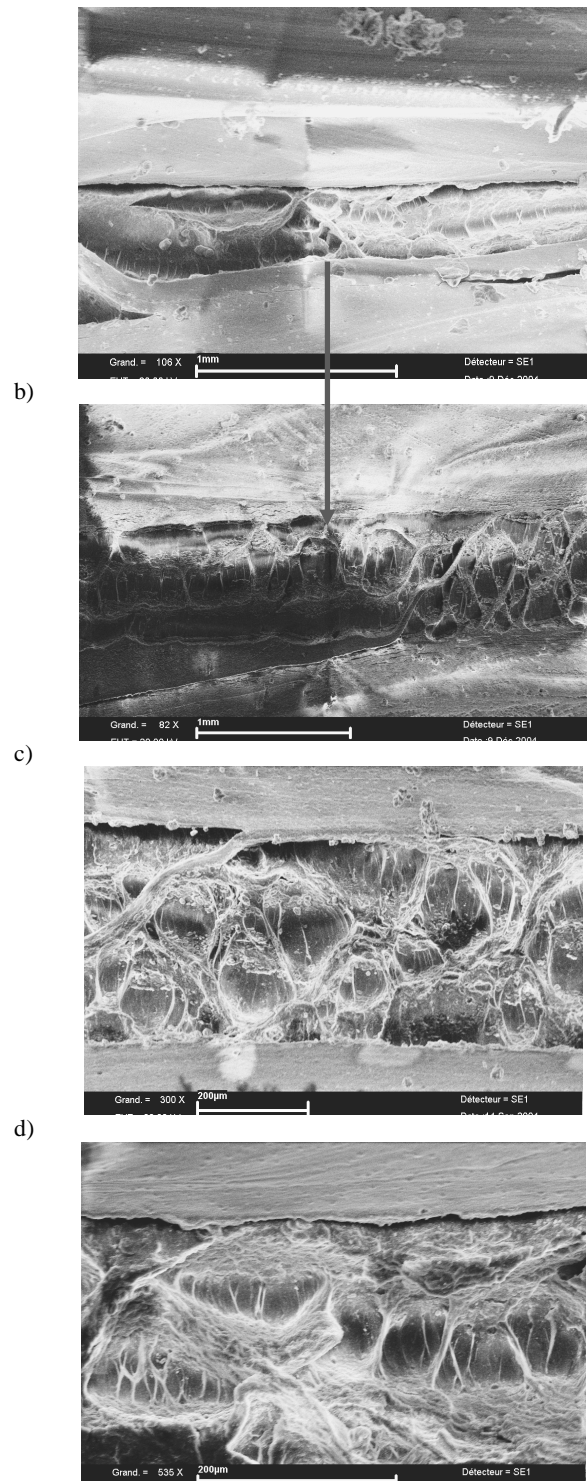


Fig. 5. SEM photomicrographs showing the beginning the damage initiation mechanism at the bottom of crack of the samples



Fig. 6. 3D Finite elements model (reflected for the sake of comprehension)



Fig. 7. Notch shape (coloured) viewed on the symmetry plane

4.1. Boundary conditions and loading

Symmetry boundary conditions have been applied on the symmetry plane (displacement $Y = 0$, rotation $X = 0$, rotation $Z = 0$) excepted for the lancet-cut surface, which is a free surface (Figure 8).



Fig. 8. Symmetry boundary conditions surfaces

A uniform normal displacement is applied on the upper face of the model at a (0.25 mm/s) steady rate from 0 to 20 mm.

4.2. Meshing

The mesh has been adapted to each notch length to ensure a reasonable stress-strain description. 3D linear tetrahedral elements were used. Modelling of the notch tips drew a particular attention, since these elements were to be most distorted along the loading process. Geometrical partition were used to enforce the meshing (free meshing procedure) to properly describe the critical zones. The meshing, for example, of the 50 mm length notched specimen required 64.185 nodes and 346.209 elements, equivalent to 192.555 degrees of freedom (same order of magnitude for all the models).

5. Comparative analysis

To compare with experimental data, force vs. displacement curves are computed from the finite elements analysis. The displacement is directly known as loading of the model and the force is obtained from the reaction force at the symmetry boundary conditions surfaces (Figure 9). A correction is made due to our modelling of only half of the specimen.

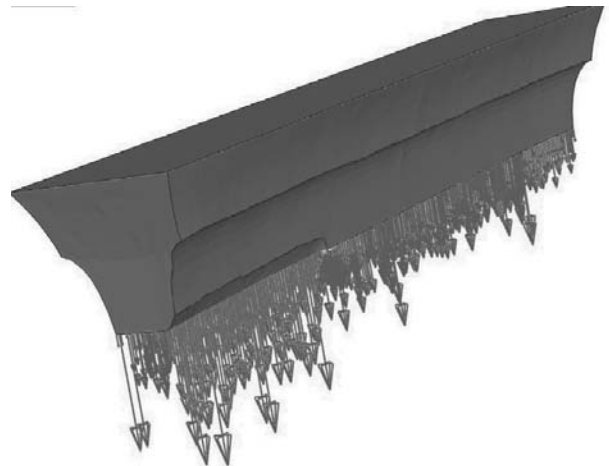


Fig. 9. Nodal reaction forces for a 50 mm notched specimen under a 7.37 mm displacement

For each length of the notch, a 14 mm displacement was applied along the 1s step time. This means that the step time parameter (ranging from 0 to 1) allows determining for each increment the applied displacement. Therefore, with one single load case, and using the results for each increment, the whole force-displacement curve was deduced (discredited using the step-time parameter).

Thus, the post-treating of the FEA gave for each displacement level with an associated total reaction force. An integration of the force-displacement curve was carried out in the Figure 10.

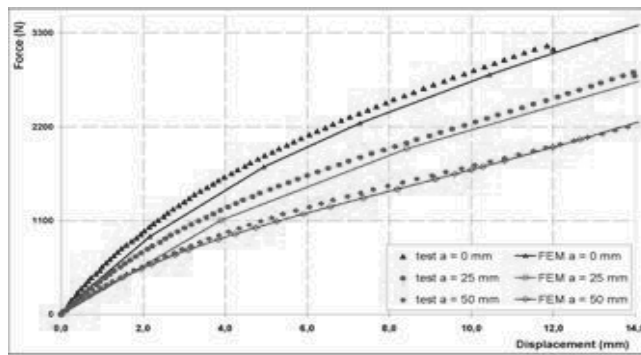


Fig. 10. Comparison of tensile test results of the NR-DCB notched specimens with different notch length

6. Conclusions

In this paper, an experimental and numerical study was carried out on the modelling of the damage initiation mechanisms in Double Cantilever Beam (DCB) specimens from natural rubber (NR) vulcanised and reinforced with other materials such as carbon black, silica, fibres and textiles or metals (rubber composites).

The FEA results have been compared with those of experimental. Some major trends can be underlined from this comparative study:

This work gives a threshold criterion for the damage just at the early beginning of the damage for the DCB specimens. The stresses are the basic reasons at the edge crack well before the final crack. Crystallisation phenomenon gives an additional effect on the damage initiation.

For the design purposes of the NR-DCB composite applications, a hyper elastic Moonley-Rivlin law and a Griffith criterion are chosen. The finite elements analysis was performed with ABAQUS code (V.6.4.4).

The comparison of experimental and numerical results has been shown to be in agreement with damage initiation in NR-DCB composites with chosen mechanical law for this damage initiation.

Acknowledgements

The authors thank Mr. M.A. Helleboid, Mr. O. Thao and Mr. R. Luong for contribution obtained during their graduating research work at LISMMA in Supmeca- Paris. Personally, E. BAYRAKTAR is indebted to Dr. P. Heuillet from LRCP-Paris for the supplying of the DCB specimens

References

- [1] R.S. Rivlin, A.G. Thomas, Rupture of Rubber. Part 1: Characteristic energy for tearing, *Journal of Polymers Sciences* 10 (1953) 291-318.
- [2] G.J. Lake, Fatigue and fracture of elastomers, *Rubber Chemical Technology* 66 (1995) 435-460.
- [3] H.W. Greensmith, The change in Stored Energy on Making a Small Cut in a Test Piece held in Simple Extension, *Journal of Polymer Science* 7 (1963) 993-1002.
- [4] P.B. Lindley, Energy for crack growth in model rubber components, *Journal Strain Analysis* 7 (1972) 132-140.
- [5] A.N. Gent, M.R. Kashani, Why do cracks turn sideways?, *Rubber Chemistry and Technology* 76 (2001) 122-131.
- [6] R. Luong, MSc, SUPMECA-Paris/LISMMA, EA-2336, St-Ouen, Paris/France, 2005.
- [7] M.A. Helleboid, O. Thao, BSc, SUPMECA-Paris/LISMMA, EA-2336, St-Ouen, Paris/France, 2006.
- [8] R. Luong, N. Isac, E. Bayraktar, Failure mechanisms in thin rubber sheet composites under static solicitation, *Journal of Achievements in Materials and Manufacturing Engineering* 21/1 (2007) 43-46.
- [9] P.V.M. Rao, S.G. Dhande, A flexible surface tooling for sheet-forming processes: conceptual studies and numerical simulation, *Journal of Materials Processing Technology* 124/1-2 (2002) 133-143.
- [10] E. Bayraktar, F. Montembault, C. Bathias, Damage Mechanism of Elastomeric Matrix Composites, *Proceedings of the "Society for Experimental Mechanics" SEM2005, Portland, 2005.*
- [11] J. Wu, J. Huang, N. Chen, C. Wei, Y. Chen, Preparation of modified ultra-fine mineral powder and interaction between mineral filler and silicone rubber, *Journal of Materials Processing Technology* 137/1-3 (2003) 40-44.
- [12] H. Ghaemi, K. Behdinin, A. Spence, On the development of compressible pseudo-strain energy density function for elastomers: Part 1. Theory and experiment, *Journal of Materials Processing Technology* 178/1-3 (2006) 307-316.
- [13] M.H. Makled, T. Matsui, H. Tsuda, H. Mabuchi, M.K. El-Mansy, K. Morii, Magnetic and dynamic mechanical properties of barium ferrite-natural rubber composites, *Journal of Materials Processing Technology* 160/2 (2005) 229-233.
- [14] R. Zulkifli, L.K. Fatt, C.H. Azhari, J. Sahari, Interlaminar fracture properties of fibre reinforced natural rubber/polypropylene composites, *Journal of Materials Processing Technology* 128/1-3 (2002) 33-37.
- [15] H. Ghaemi, K. Behdinin, A. Spence, On the development of compressible pseudo-strain energy density function for elastomers: Part 2. Application to FEM, *Journal of Materials Processing Technology* 178/1-3 (2006) 317-327.
- [16] R.M.V. Pidaparti, Finite element analysis of interface cracks in rubber materials, *Journal of Engineering Fracture Mechanics* 47/2-3 (1994) 309-316.
- [17] R.M.V. Pidaparti, T.Y. Yang, W. Soedel, A plane stress FEA for the prediction of rubber fracture, *International Journal of Fracture* 39 (1989) 255-268.
- [18] W.V. Mars, A. Fatemi, Multiaxial stress effects on fatigue behaviour of filled natural rubber, *Journal of Fatigue* 28/5 (2006) 521-529.